J|A|C|S
ARTICLES

Published on Web 09/20/2008

Water Phase Transition Induced by a Stone−Wales Defect in a Boron Nitride Nanotube

Chang Y. Won and N. R. Aluru*

Department of Mechanical Science and Engineering, Beckman Institute for Advanced Science and Technology, University of Illinois at Urbana−Champaign, Urbana, Illinois 61801

Received May 8, 2008; E-mail: aluru@illinois.edu

Abstract: Boron nitride nanotubes (BNNTs) have been reported to possess superior water permeation properties. In this work, using molecular dynamics simulations with partial charges, capturing BNNT polarization effects obtained from quantum calculations, we found that Stone−Wales (SW) defects in a (5,5) BNNT result in phase transition of water, i.e., a transition between liquid-like phase and vapor-like phase was observed. The 90° rotation of the B−N bond, SW transformation, in an SW-defective (5,5) BNNT results in breaking of hydrogen bonding with neighboring water molecules and leads to the existence of a vapor-like phase near the SW defect. Water transport rate was evaluated by measuring translocation time. Water in an SW-defective (5,5) BNNT has fewer translocation events, longer translocation time, and a higher axial diffusion coefficient compared to water in a nondefective (5,5) BNNT.

Introduction

Subnanometer nanotubes immersed in an ionic solution have been studied extensively over the past decade due to their wide range of applications in biological/chemical systems,[1,2] fuel cell devices,[3] etc. Boron nitride nanotubes (BNNTs), because of their superior electrical,[4] physical,[5,6] and chemical properties,[7] have been considered as a promising material for the applications mentioned above. Recently, Won and Aluru[8] showed that a BNNT exhibits superior water-filling behavior because of the comparatively strong interactions between nitrogen atoms on a BNNT and water molecules. The formation of hydrogen bonds between the confined water and nitrogen atoms on the BNNT can markedly influence the structure and dynamical properties of water inside the tube.[9] Most theoretical studies on water and nanotubes have been performed using nondefective nanotubes. However, experimental studies have indicated that BNNTs can have defects in the structure. For example, Stone−Wales (SW) defect[10] is shown to be present in a BNNT under tension[11] and can be observed spectroscopically.[12] Previous studies[13,14] on SW defect in BNNTs revealed its effects on the nanotube's electronic properties and H_2 absorption. However, many other effects, including the effect of the defects on water structure and transport, are not known. In this work, we report that water phase shifts from liquid-like phase to vapor-like phase and vice versa in a finite length (5,5) BNNT in the presence of an SW defect.

Simulation Methods

To evaluate the effect of the SW defect on water behavior inside the BNNT, we perform quantum and molecular dynamics (MD) simulations on two finite length (5,5) nondefective and SW-defective BNNTs with a diameter of 6.9 Å and a length of approximately 26.2 Å. Both tubes are saturated at the ends with hydrogen atoms. The SW defect is located in the middle of the BNNT. The initial BN bond length was 1.446 Å. The N−H and B−H bond length was 1.09 Å. The nitrogen atoms were then moved slightly outward (by ∼0.032 Å), and the boron atoms were moved slightly inward from the tube center (by ∼0.032 Å), to make a buckled BNNT, which is consistent with previous ab initio calculations on BNNT geometries.[15,16] We then obtained geometry-optimized structures for both tubes by the AM1 semiempirical method using Gaussian 03.[17] For BNNT geometries, the AM1 method reproduces the large cBN cluster in good agreement with the experimental structure.[18]

Quantum partial charges, accounting for polarization of the nanotube due to the weak ionic and covalent bonding of B−N and the polarization of the nanotube because of nanotube−water

(1) Weik, M.; Lehnert, U.; Zaccai, G. *Biophys. J.* **2005**, *89*, 3639.
(2) Murata, K.; Mitsuoka, K.; Hirai, T.; Walz, T.; Agre, P.; Haymann, J. B.; Engel, A.; Fujiyoshi, Y. *Nature* **2000**, *98*, 1398.
(3) Wang, Z.; Medforth, C. J.; Shelnutt, J. A. *J. Am. Chem. Soc.* **2004**, *126*, 16720.
(4) Blasé, X.; Bubbio, A.; Louie, S. G.; Cohen, M. L. *Europhys. Lett.* **1994**, *28*, 335.
(5) Chopra, N. G.; Zettl, A. *Solid State Commun.* **1998**, *105*, 297.
(6) Chang, C.; Han, W.-Q.; Zettl, A. *J. Vac. Sci. Technol., B* **2005**, *23*, 1883.
(7) Chen, Y.; Zou, J.; Campbel, S. J.; Caer, G. L. *Appl. Phys. Lett.* **2004**, *84*, 2430.
(8) Won, C. Y.; Aluru, N. R. *J. Am. Chem. Soc.* **2007**, *129*, 2748.
(9) Won, C. Y.; Aluru, N. R. *J. Phys. Chem. C* **2008**, *112*, 1812.
(10) Stone, A.; Wales, D. *Chem. Phys. Lett.* **1986**, *128*, 501.
(11) Bettinger, H. F.; Dumitricä, T.; Scuseria, G. E.; Yakobson, B. I. *Phys. Rev. B* **2002**, *65*, 041406.
(12) Miyamoto, Y.; Rubio, A.; Berber, S.; Yoon, M.; Tománek, D. *Phys. Rev. B* **2004**, *69*, 121413.
(13) Wu, X.; Yang, J.; Hou, J. G.; Zhu, Q. *J. Chem. Phys.* **2006**, *124*, 054706.
(14) Li, Y.; Zhou, Z.; Golberg, D.; Bando, Y.; von Ragué Schleyer, P.; Chen, Z. *J. Phys. Chem. C* **2008**, *112*, 1365.
(15) Wirtz, L.; Rubio, A.; de la Concha, R. A.; Loiseau, A. *Phys. Rev. B* **2003**, *68*, 045425.
(16) Akdim, B.; Pachter, R.; Duan, X.; Adams, W. W. *Phys. Rev. B* **2003**, *67*, 245404.
(17) Frisch, M. J.; et al. Gaussian 03, revision C. 02; Gaussian, Inc.: Wallingford, CT, 2004.
(18) Komatsu, S.; Yarbrough, W.; Moriyoshi, Y. *J. Appl. Phys.* **1997**, *81*, 7798.

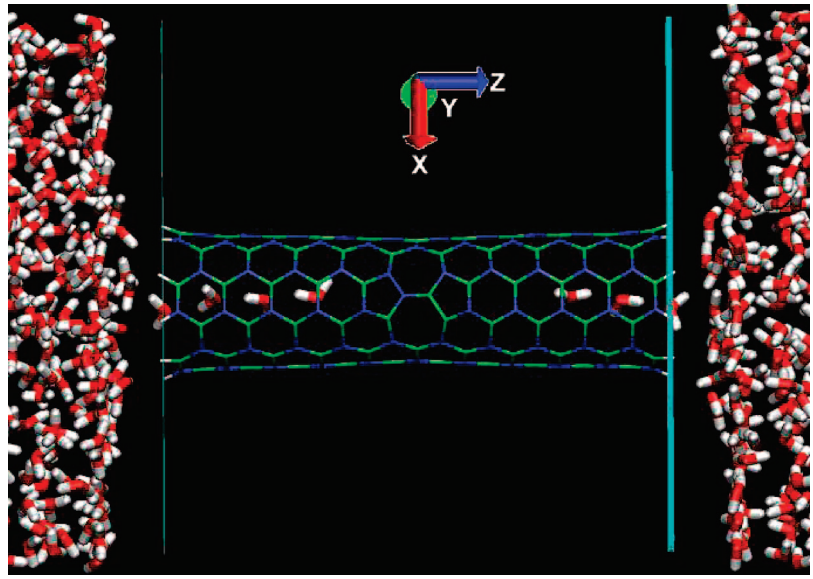

Figure 1. Visualization of a broken single-file water chain in a (5,5) BNNT with Stone−Wales (SW) defects in the center of the tube.

interaction, were computed by density functional theory (DFT) calculations. Gaussian 03[17] was used for the DFT calculations with B3LYP/6-31G** on the geometry-optimized structures. The partial charges on the tubes were obtained by fitting the electrostatic potential to fixed charges on the boron, nitrogen, and hydrogen atoms using the CHelpG scheme.[19] The CHelpG charges based on a molecular electrostatic potential are suited for MD simulations as they can capture higher order effects arising from dipoles and multipoles, though in an approximate way. We verified our partial charge calculations by comparing the magnitude of partial charges of H atoms forming dangling bonds with B and N atoms at the end of a tube with previous DFT calculations for H atoms bonding with a B−N cluster.[20] We found a good agreement between our partial charge calculations with the previous calculations. To investigate the effect of water molecules on the tube partial charges, we performed DFT calculations based on four different representative configurations obtained from equilibrium MD simulations that consisted of the nanotube and water molecules inside the tube and near the tube entrance. Two of the configurations were obtained from the MD simulations without partial charges on the atoms. The other two configurations were obtained by including partial charges on the atoms in MD simulations. Due to the inhomogeneous distribution of water molecules along the tube axial direction, the partial charge distribution is not quite symmetric with respect to the center of the nanotube.

The quantum partial charges are included in the MD simulation. For MD simulations, the nanotube is fixed in a slab and water reservoirs are attached to the nanotube on either end (see Figure 1). The initial simulation box was $2.8 \times 2.772 \times 7.00$ nm^3. The reservoirs were initially filled with approximately 1020 water molecules. Water is modeled by using the extended simple point charge (SPC/E) model.[21] The SETTLE algorithm was implemented to constrain the OH bond length and the HOH bond angle at 1.0 Å and 109.47°, respectively. The simulations were performed for 19 ns with a 1.0 fs time step by using modified GROMACS 3.3.1.[22] The Nosé−Hoover thermostat[23] with a time constant of 0.1 ps was employed to regulate the temperature at 300 K. The Parrinello−Rahman piston-coupling scheme[24] with a time constant of 2.0 ps and a compressibility of 4.5×10^{-5} bar^{-1} maintained the system at 1 bar along the nanotube axial direction, which results in adjustment of the simulation box size in the tube axial direction. The Lennard-Jones (LJ) parameters for the boron and nitrogen atoms were taken from ref 25 ($\sigma_{B-B} = 0.3453$ nm, $\varepsilon_{B-B} = 0.3971$ kJ/mol, $\sigma_{N-N} = 0.3365$ nm, $\varepsilon_{N-N} = 0.6060$ kJ/mol), and parameters for the saturated hydrogen atoms were taken from ref 26 ($\sigma_{H-H} = 0.2813$ nm, $\varepsilon_{H-H} = 0.0683$ kJ/mol). Particle mesh Ewald (PME) method with a 10 Å real-space cutoff, 1.5 Å reciprocal space gridding, and splines of order 4 with a 10^{-5} tolerance was implemented to compute electrostatic interactions. The equations of motion were integrated by using a leapfrog algorithm, and the simulation time step is 1.0 fs.

Results and Discussion

The (5,5) BNNTs were initially empty. Water molecules from the water reservoir quickly filled the empty nondefective nanotube by forming a single-file chain similar to the water structure observed in previous study.[9] Once the nanotube is filled, during most of the simulation time, approximately nine water molecules inside the BNNT continuously formed a single-file water chain. The SW-defective BNNT has a substantially different water-filling behavior compared to the nondefective nanotube; especially the water structure near the SW defect is different. Unlike in the nondefective BNNT, the single-file water chain was not continuously observed in the SW-defective BNNT. The single-file water chain often breaks near the SW defect, which leaves an empty region as shown in Figure 1. Analogous to the previously used definition[27] of a vapor-like phase of water in a 0.8 nm long nanopore, we use the following definition to identify the phase of water in a subnanometer nanotube: liquid-like phase when the nanotube is completely filled with water molecules and the distance between nearest water molecules is less than 0.75 nm which is slightly larger than twice the O—O distance used in the hydrogen-bonding

(19) Breneman, C. M.; Wiberg, K. B. *J. Comput. Chem.* **1990**, *11*, 361.
(20) Han, S. S.; Kang, J. K.; Lee, H. M.; van Duin, A. C. T.; Goddard, W. A. *J. Chem. Phys.* **2005**, *123*, 114703.
(21) Berendsen, H. J. C.; Grigera, J. R.; Straatsma, T. P. *J. Phys. Chem.* **1987**, *97*, 6269.
(22) Lindahl, E.; Hess, B.; van der Spoel, D. *J. Mol. Model.* **2001**, *7*, 306.
(23) Hoover, W. *Phys. Rev. A* **1985**, *31*, 1695.
(24) Parrinello, M.; Rahman, A. *J. Appl. Phys.* **1981**, *52*, 7182.
(25) Kang, J. W.; Hwang, H. J. *J. Phys.: Condens. Matter* **2004**, *16*, 3901.
(26) Murad, S.; Gubbins, K. E. *ACS Symp. Ser.* **1978**, *86*, 62.
(27) Beckstein, O.; Sansom, M. S. P. *Proc. Natl. Acad. Sci. U.S.A.* **2003**, *100*, 7063.

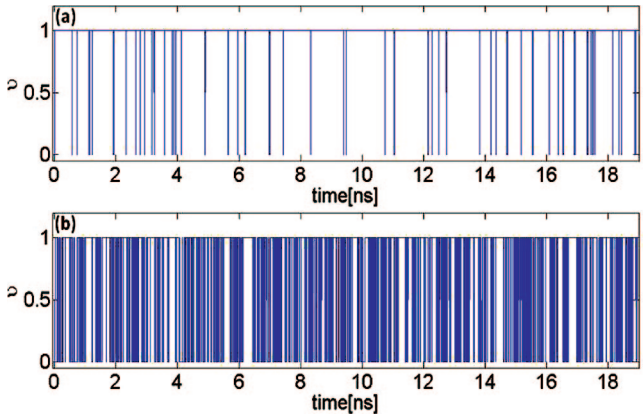

Figure 2. Phase transition $\upsilon(t)$ of water inside the (a) nondefective and (b) SW-defective (5,5) boron nitride nanotube (BNNT).

criteria. Otherwise, we define a vapor-like phase. Even though we refer to the broken chain as vapor-like phase, other interpretations such as cavity, nanobubble, or a broken chain also would be a reasonable interpretation. To measure the frequency of the phase transition, we assign $\upsilon(t) = 1$ for liquid-like phase and $\upsilon(t) = 0$ for vapor-like phase. The vapor-like phase in the nondefective nanotube was observed to be only 0.81% of the entire simulation time (Figure 2a). In contrast, in the defective nanotube the vapor-like phase was observed to be 23.52% of the total simulation time (Figure 2b).

The different water phase behavior in the nondefective and SW-defective BNNTs was understood by decomposing the total force field into LJ and electrostatic force fields. We performed MD simulations without including nanotube polarization effects, i.e., by assigning zero partial charge to all the atoms of the tube. In this case, we found that liquid-like phase is most favorable inside SW-defective BNNT. The vapor-like phase of water was observed during approximately 0.42% of simulation time. Further analysis revealed that the partial charges arising from the SW defect and the partial charges arising from the nanotube−water interaction are both important in inducing the phase transition. Figure 3 shows the averaged partial charges for the atoms with the same axial position. The SW transformation, 90° rotation of B−N bond, adds considerable dipole effect in the middle of the nanotube (see Figure 3a). The partial charges of boron and nitrogen atoms in the SW defect are $0.29e$ and $-0.33e$, respectively. In the absence of SW defect, there is no dipole effect in the middle of the nanotube as shown in Figure 3b. Water orientation in the BNNT is primarily determined by orientations of water near both ends due to the combination of dominant tube end effects and strong water−water hydrogen bonding.[9] The presence of a considerable dipole effect in the SW-defective nanotube significantly influences the orientation of water molecules near the defect. Thus, water molecules near the SW defect experience the competition from neighboring water orientation affected by the end effects and from the dipole near the center of the nanotube. As a result, water located near the SW defect has higher chance to lose hydrogen bonding with neighbor water molecules. Vapor-like phase is then induced in the SW-defective BNNT.

We then investigated the effect of SW defect on water transport properties. The water transport rate was measured by computing the translocation time. The translocation time is defined as the time taken for water molecules to travel from one end of the tube to the other end of the tube. We observed that on an average 2.72 water molecules/ns translocated through

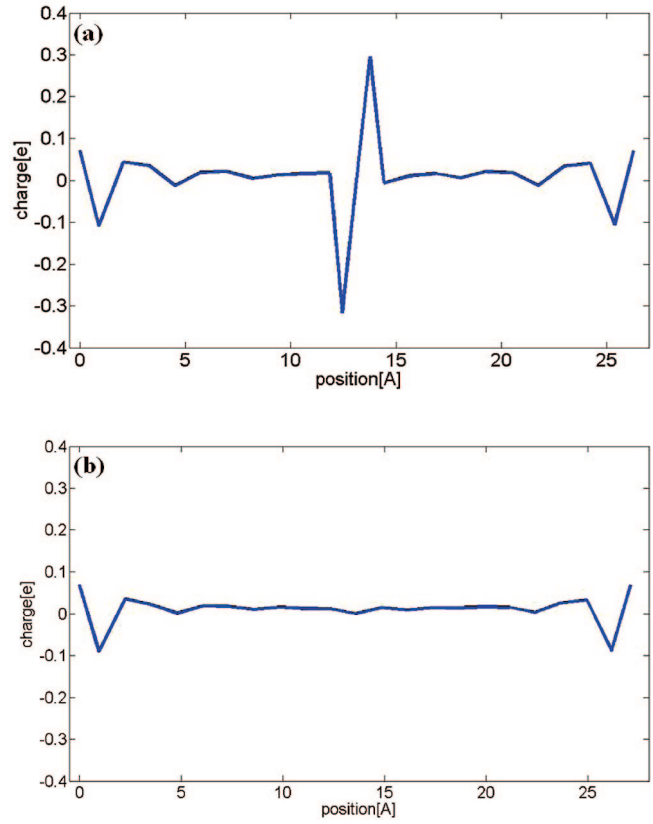

Figure 3. Partial charge distribution for atoms on SW-defective (5,5) boron nitride nanotube (BNNT) (a) and on a nondefective (5,5) BNNT (b) along the tube axial direction. The BNNT starts at 0 Å in the axial direction.

the nondefective BNNT with a translocation time average of 1.26 ns. In the case of defective nanotube, about 1.22 water molecules/ns cross the BNNT with an average translocation time of 1.55 ns. Even though the transport rate is diminished, the SW-defective BNNT exhibited a higher diffusion coefficient compared to the nondefective BNNT. The axial diffusion coefficient D_z of water is related to the slope of the water mean-squared displacement (MSD) by the well-known Einstein relation

$$D_z = \frac{1}{2}\lim_{t\to\infty}\frac{\langle |r(t) - r(0)|^2\rangle}{\Delta t} = \frac{1}{2}\lim_{t\to\infty}\frac{\langle \Delta r^2\rangle}{\Delta t} \qquad (1)$$

where $r(t)$ is the position vector at time t. The axial diffusion coefficient of water in SW-defective BNNT was found to be 1.36×10^{-5} cm^2/s, which is about 18.26% higher than water diffusion in a (5,5) nondefective BNNT reported recently.[9]

The discrepancy between the axial diffusion coefficient and the transport rate can be explained by computing the water residence time and the axial motion of water molecules in the nanotube. We evaluated the residence time of water and the probability for the direction of water movement in a nanotube by using the binning method. The entire simulation box was binned along the nanotube axial direction. The width of each bin is similar to the size of one water molecule, 2.2 Å. For the residence time, we measured the average time of water molecules in a bin. When water molecules travel from the current bin to the neighbor bin, the direction of water motion as well as its probability is computed. Figure 4 shows that the residence time of water in both tubes is higher at the ends compared to the middle region. An L-defect in the single-file chain is observed for both cases. Because of the formation of

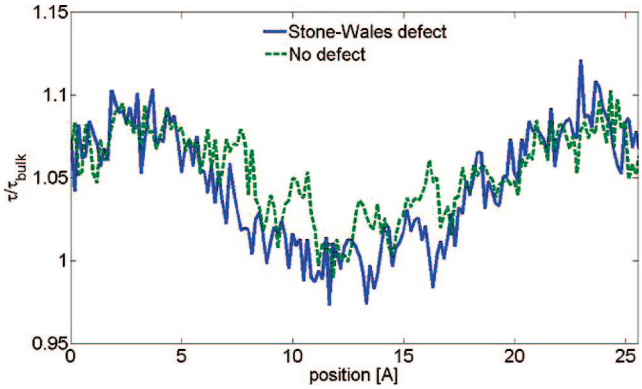

Figure 4. Residence time of water along the tube axial direction in the nondefective (dashed line) and SW-defective (solid line) (5,5) BNNT. The BNNT starts at 0 Å in the axial direction.

L-defect in the middle of the BNNT, water−water electrostatic interaction is less favorable,[28] which leads to smaller residence time for water in the middle of a BNNT. In the case of SW-defective BNNT, the presence of the vapor-like state in the middle further lowers the residence time (Figure 4). We then evaluated the probability of water movement along the tube axial direction. Water molecules in a nondefective (5,5) BNNT have similar probability of moving forward or backward along the tube axial direction. For defective BNNT, water molecules near the tube ends have similar probability of moving forward or backward along the tube axial direction. However, water molecules in the location where the vapor-like state can be observed have approximately 50% higher probability of moving toward their nearest tube end. These observations suggest that water molecules inside the SW-defective BNNT have higher oscillatory motion between the tube end and the SW defect location, which results in a higher diffusion coefficient and a smaller number of translocation events.

We also investigated the effect of flexibility or polarizability of the water model on the single-file water phase transition in the SW-defective BNNT since these effects are not included in the rigid nonpolarizable SPC/E water model. The flexibility is included by adding internal (bond stretching and angle bending) conformational change to the SPC/E water model.[29] For polarizable water model, the SWM4-DP water model[30] was implemented in the MD simulation. With the flexible and polarizable water model, we observed similar phenomena as with the rigid nonpolar SPC/E water models: continuous single-file water phase transition between liquid-like and vapor-like states and low translocation rate of water molecules inside the SW-defective BNNT.

Conclusion

The results presented in this paper suggest that an SW defect in a (5,5) BNNT can induce phase transition of water from liquid-like phase to vapor-like phase. The vapor-like phase can be observed near the location of the SW defect. By decomposing the total force field into LJ and electrostatic force fields, we found that the partial charges arising from both the SW defect and the nanotube−water interaction play an important role in the formation of vapor-like state inducing the phase transition. The presence of an SW defect introduces a dipole in the middle of a (5,5) BNNT. In the presence of the dipole, water molecules near the SW defect have a higher chance of breaking hydrogen bonding with neighbor water molecules, due to the competition from neighboring water orientation affected by the end effects and from the dipole near the center of the nanotube. Water transport rate decreases with the SW defect, but the high oscillatory motion of water in the tube axial direction gives rise to a larger diffusion coefficient.

Acknowledgment. This research was supported by the NSF under Grant Nos. 0328162, 0120978, 0523435, and 0625421 and by the NIH under Grant No. PHS 2 PN2 EY016570B.

Supporting Information Available: Details on the structure of a (5,5) SW-defective BNNT and complete ref 17. This material is available free of charge via the Internet at http://pubs.acs.org.

JA803245D

(28) Won, C. Y.; Joseph, S.; Aluru, N. R. *J. Chem. Phys.* **2006**, *125*, 114701.
(29) Ferguson, D. M. *J. Comput. Chem.* **1995**, *16*, 501.
(30) Lamoureux, G.; Mackerell, A. D., Jr.; Roux, B. *J. Chem. Phys.* **2003**, *119*, 5185.